ANNUAL REVIEWS

Annual Review of Physiology

Metabolic Recruitment in Brain Tissue

L.F. Barros,[1,2] I. Ruminot,[1,2] T. Sotelo-Hitschfeld,[3] R. Lerchundi,[4] and I. Fernández-Moncada[5]

[1]Centro de Estudios Científicos (CECs), Valdivia, Chile; email: fbarros@cecs.cl

[2]Facultad de Medicina y Ciencia, Universidad San Sebastián, Valdivia, Chile; email: luis.barros@uss.cl

[3]Department of Neuronal Control of Metabolism, Max Planck Institute for Metabolism Research, Cologne, Germany

[4]Commissariat à l'Energie Atomique et aux Energies Alternatives (CEA), MIRCen, Fontenay-aux-Roses, France

[5]NeuroCentre Magendie, INSERM U1215, University of Bordeaux, Bordeaux, France

Annu. Rev. Physiol. 2023. 85:115–35

First published as a Review in Advance on October 21, 2022

The *Annual Review of Physiology* is online at physiol.annualreviews.org

https://doi.org/10.1146/annurev-physiol-021422-091035

Keywords

neurons, astrocytes, glucose, lactate, oxygen, glycolysis, mitochondria

Abstract

Information processing imposes urgent metabolic demands on neurons, which have negligible energy stores and restricted access to fuel. Here, we discuss metabolic recruitment, the tissue-level phenomenon whereby active neurons harvest resources from their surroundings. The primary event is the neuronal release of K^+ that mirrors workload. Astrocytes sense K^+ in exquisite fashion thanks to their unique coexpression of NBCe1 and $\alpha 2\beta 2$ Na^+/K^+ ATPase, and within seconds switch to Crabtree metabolism, involving GLUT1, aerobic glycolysis, transient suppression of mitochondrial respiration, and lactate export. The lactate surge serves as a secondary recruiter by inhibiting glucose consumption in distant cells. Additional recruiters are glutamate, nitric oxide, and ammonium, which signal over different spatiotemporal domains. The net outcome of these events is that more glucose, lactate, and oxygen are made available. Metabolic recruitment works alongside neurovascular coupling and various averaging strategies to support the inordinate dynamic range of individual neurons.

INTRODUCTION

ANLS: astrocyte-to-neuron lactate shuttle; a model of brain metabolic coupling in which glutamate released by neurons stimulates astrocytic glycolysis and lactate production

NKA: Na^+/K^+ ATPase; a pump that modulates glycolysis and mitochondrial respiration by unknown mechanisms

The metabolic rate is the speed at which cells live. It varies from cell to cell and from one moment to the next. It drops during sleep and rises when tissues are active, for example, during exercise for muscle, heart, and brain, or during food processing for the gut, liver, and fat. Every cell is equipped with homeostatic devices that adjust adenosine 5′-triphosphate (ATP) production to workload. This coupling may be so smooth that excitable cells may raise their work rate without detectable ATP depletion (1–3).

In relatively homogeneous organs such as heart and skeletal muscle, adjacent cells play similar roles. In the brain, adjacent cells behave differently. Neurons transit time and again between resting and activity and, in the process, are forced to deal with incremental energy demands that reach orders of magnitude (4, 5). Neurons do not have sizable energy stores and must constantly be supplied with fuel. Interposed between them and blood-borne nutrients are astrocytes (6, 7), which store glycogen, a polymer of glucose that is the organ's main energy reservoir (8, 9). In brain tissue the metabolic response is not just the algebraic sum of individual cell adaptations, but a higher-order phenomenon involving the division of labor between cell types (10–13). An early example of metabolic cooperation between cells is the astrocyte-to-neuron lactate shuttle (ANLS), the stimulation of astrocytic glucose consumption and lactate production mediated by the Na^+/glutamate cotransporter (14, 15). The ability of glutamate, acting via its transporter, to impact the metabolism of astrocytes is modest compared to that of K^+. Only three Na^+ ions enter the cell with each glutamate, a small number relative to the 150 Na^+ ions that are extruded per glutamate in exchange with K^+ at the astrocytic Na^+/K^+ ATPase (NKA), as detailed below. Another shortcoming of extracellular glutamate as a metabolic signal is poor correlation with workload. The extracellular concentration of glutamate may be a good proxy of the energy demand of synaptic boutons, but because of variable inhibitory input, it does not correlate well with the activity of dendrites and somata, where most of the energy is consumed (5, 16, 17), or with the metabolic demand at nonglutamatergic excitatory synapses. A third limitation is reach. Glutamate is extremely local, sensed by a single astrocyte (18); there is also the issue of speed. The glycolytic effect of glutamate on astrocytes takes minutes to kick in (19), too late to cater to the ATP demand of neurons, which peaks seconds after neurotransmission (1, 20, 21).

In this review, we argue that active neurons harvest glucose, lactate, and oxygen from astrocytes and neurons located beyond the active zone and that the main signal driving this fast metabolic recruitment is extracellular K^+ ($[K^+]_e$). The case for potassium-mediated recruitment rests on five pillars: (*a*) Elevated $[K^+]_e$ is a mirror of workload across the brain; (*b*) elevated $[K^+]_e$ reaches astrocytes beyond the active zone; (*c*) astrocytes are uniquely endowed to sense $[K^+]_e$; (*d*) the metabolism of astrocytes is acutely modulated by $[K^+]_e$; and (*e*) the metabolism of astrocytes and neurons is modulated by lactate, which serves as a secondary recruiter.

$[K^+]_e$ MIRRORS WORKLOAD

The excitatory postsynaptic potential, the main electric signal employed by neurons to pass information, is mediated by the influx of Na^+ and Ca^{2+} through α-amino-3-hydroxy-5-methyl-4-isoxazolepropionic acid (AMPA) and *N*-methyl-D-aspartate (NMDA) ionotropic glutamate receptors. Most of the Ca^{2+} load is swiftly transformed into a Na^+ load by the Na^+/Ca^{2+} exchanger, and the Na^+ gradient is then restored by the NKA, the dominant energy sink of brain tissue (5, 16). In comparison, the energy consumption of axons and glial cells has been deemed modest (17; but see 22). What is sometimes overlooked is that AMPA and NMDA receptors conduct K^+ and that additional K^+ is released by active neurons through Ca^{2+}- and voltage-gated K^+ channels (23). In fact, electroneutrality dictates that the release of K^+ matches the entry of

Na^+ at approximately 100 ions per exocytosed glutamate (5). Therefore, $[K^+]_e$ amplifies the glutamate signal by two orders of magnitude, and because K^+ efflux is inextricably coupled to the entry of Na^+ that will be pumped out later on, the transformation of a presynaptic glutamate signal into an amplified postsynaptic extracellular K^+ signal proceeds only if neurons require energy. This obligatory link existing between release and workload distinguishes K^+ from glutamate. If glutamate fails to evoke a postsynaptic current because of coincident inhibitory input like gamma-aminobutyric acid (GABA) or ATP-sensitive potassium channel (K_{ATP}) activation, there will be no Na^+ entry and workload, but astrocytes will still have to deal with the glutamate and GABA. Resting $[K^+]_e$ concentration is low, and therefore the release of K^+ can cause a significant elevation of $[K^+]_e$.

The dynamics of $[K^+]_e$ in brain tissue have been extensively characterized with microelectrodes and microdialysis probes, ex vivo and in vivo, most recently in awake animals (24–26). The blood–brain barrier permits autonomous regulation of brain $[K^+]_e$, shielded from plasma fluctuations induced by exercise and food absorption. At 2.5–3 mM, the lowest $[K^+]_e$ is observed during deep sleep and anesthesia, ~40% lower than in plasma. Awakening elevates $[K^+]_e$ by 0.4–0.7 mM (27), and the transition from quiescence to locomotion adds an additional 0.7–1 mM, detected not just in motor cortex but in all cortical areas tested (26). These elevations occur within seconds and correlate with increased network activity (**Figure 1*a***). Confirming a synaptic source, pharmacological blockage of excitatory neurotransmission inhibited the rise of $[K^+]_e$ induced by locomotion. On top of these cortex-wide state-dependent plateaus, transient $[K^+]_e$ elevations have been induced by a variety of paradigms (**Figure 1*b***). For physiological stimuli, surges amount to 0.2–3 mM, reaching up to 12 mM during seizures, and a maximum of 60 mM in spreading depression (**Figure 1*c***). A recent study based on genetically encoded voltage indicators indicates that local $[K^+]_e$ may reach up to 10 mM around perisynaptic astrocytic processes (28).

ELEVATED $[K^+]_e$ REACHES DISTANT ASTROCYTES

Over the sluggish timescale of metabolic events, glutamate and K^+ may be said to arrive in the synaptic cleft simultaneously, but after that, their dynamics depart dramatically. While glutamate is removed within 1 ms, K^+ diffuses for approximately 1–10 s (24, 29). Considering tissue tortuosity, diffusion coefficient, and diffusion half-time (24), K^+ is estimated to travel 80–100 μm on average. This calculation fits the $[K^+]_e$ profile recorded with an electrode stepped through the hippocampus (**Figure 1*d***). The removal of glutamate within 0.5–1 μm of the synaptic cleft (18) permits synaptic autonomy and is made possible by the combination of vanishingly low resting extracellular glutamate concentration and massive expression of Na^+/glutamate cotransporters in astrocytes. These transporters are slow (70 ms per cycle) but they remove efficiently by trapping their ligand like sticky fly paper. Their resting occupancy is near zero, and there are enough of them around each synapse to handle the maximum speed of glutamate exocytosis (30). In contrast, K^+ leaves the synaptic region unscathed. Whereas 100 K^+ ions are released per glutamate, the astrocytic NKA, which is the main mechanism clearing synaptic and axonal K^+ (31–35), is 100 times less abundant than the glutamate transporter (30, 36), a compounded factor of 10,000!

The strikingly different dynamics of glutamate and K^+ are reflected in the behavior of astrocytic Na^+. The three Na^+ ions imported per glutamate by the Na^+/glutamate cotransporter are very few compared to the 150 Na^+ ions that would need to be extruded if all synaptic K^+ ions were pumped by the NKA in the same local astrocyte that took up the glutamate. Nonetheless, in hippocampal astrocytes and cerebellar Bergmann glia exposed to glutamatergic activity, intracellular Na^+ increases, a rise mediated by the Na^+/glutamate cotransporter (37, 38). This observation confirms that, in the cells that take up all the glutamate, the NKA captures very little of the K^+.

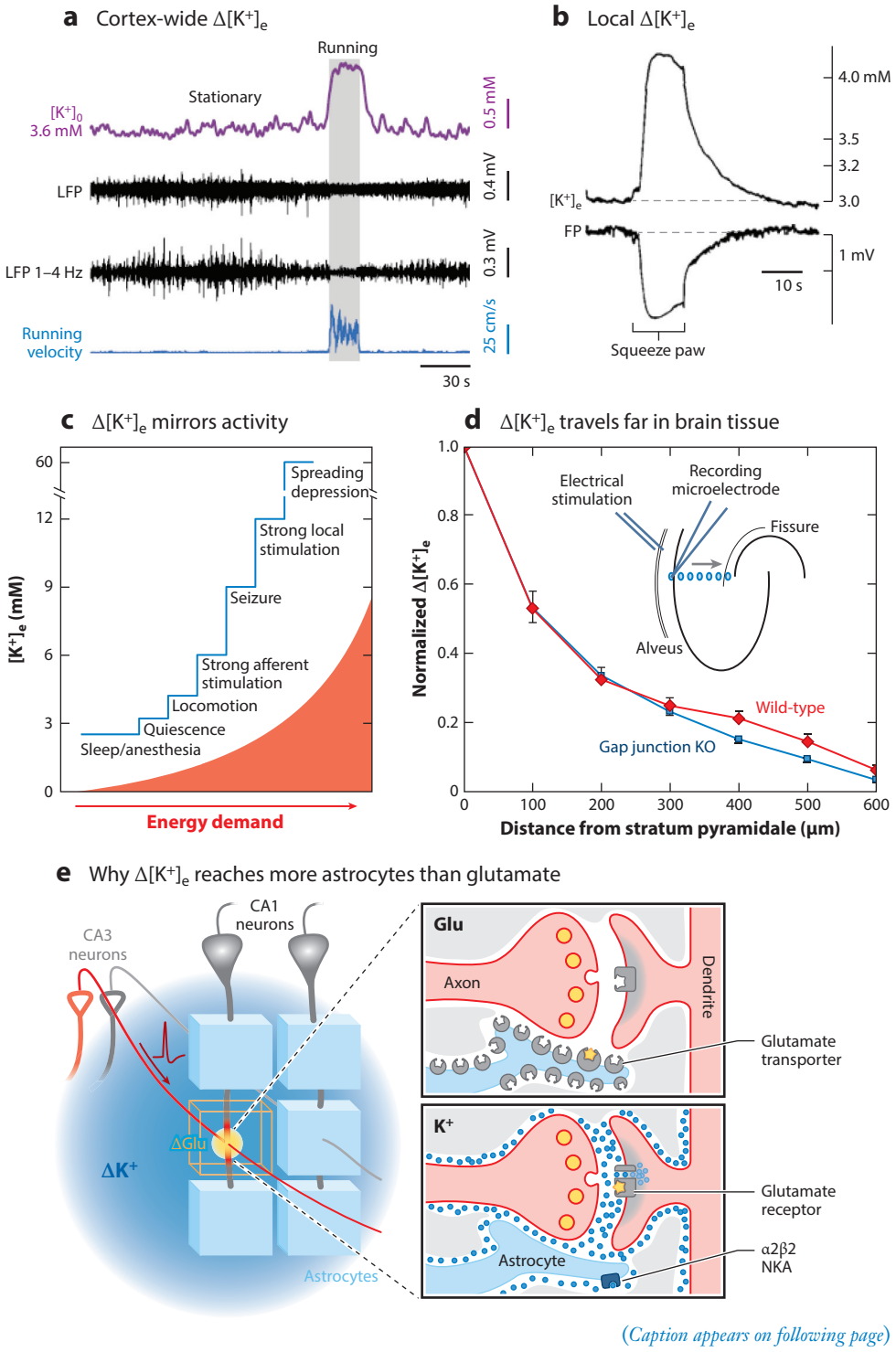

(Caption appears on following page)

Figure 1 (*Figure appears on preceding page*)

Extracellular K^+ ($[K^+]_e$) dynamics in nervous tissue. (*a*) Motor cortex $[K^+]_e$, local field potential (LFP), and velocity of a mouse before, during, and after running on a treadmill. Panel adapted with permission from Reference 26; copyright 2019 Elsevier. (*b*) Spinal cord $[K^+]_e$ and field potential (FP) in response to a noxious stimulus in an anesthetized cat. Panel adapted from Reference 132 (CC BY 4.0). (*c*) $[K^+]_e$ correlates with the degree of neural activity and the energy demand of the tissue across physiological to pathophysiological conditions. (*d*) Antidromical axonal K^+ release was triggered by electrical stimulation of the hippocampal alveus in the presence of synaptic blockers. $[K^+]_e$ was measured with a recording microelectrode stepped at 100-μm intervals from the stratum pyramidale to the hippocampal fissure. Note the minor impact of connexin 30 and 43 genetic deletion [gap junction knockout (KO)] versus wild-type on the diffusion profile. Panel adapted from Reference 53; copyright 2006 Society for Neuroscience. (*e*) Representation of the hippocampal neuropil, where Schaffer collateral axons from CA3 pyramidal neurons make synaptic contact with dendrites from CA1 pyramidal neurons. While extracellular glutamate (Glu) is cleared by a small part of a single astrocyte (*orange box*), the $[K^+]_e$ rise reaches many astrocytes (*blue boxes*). (*e*, *inset*) Glu (*top*) is quickly captured by astrocytic Glu transporters. When an ionotropic glutamate receptor is engaged, ∼100 K^+ ions are released for each Glu that is exocytosed (*bottom*). Astrocytes have ∼100 times fewer Na^+/K^+ ATPase (NKA) pumps than glutamate transporters. The compounded 10,000 factor explains why glutamate is captured locally while most K^+ diffuses away.

Thus, while all the glutamate released at a given synapse is captured by the astrocyte that wraps that synapse, most K^+ is handled by distant astrocytes (**Figure 1*e***).

EXQUISITE $[K^+]_e$ SENSING BY ASTROCYTES

Seconds after successful excitatory neurotransmission, a wave of K^+ reaches the surface of astrocytes. High expression of constitutively open K^+ channels and a lack of other significant ion permeabilities makes these cells virtual Nernstian electrodes (24, 25, 39) (**Figure 2*a***). The ensuing depolarization of the astrocytic plasma membrane engages the NKA and the Na^+/bicarbonate cotransporter.

The clearance of synaptic K^+ by astrocytes instead of neurons is explained by NKA subtype allocation (33, 40–42) (**Figure 2*b***). The neuronal NKA (α3β1) does not respond well to K^+ because its high-affinity site is permanently saturated, but it is sensitive to intracellular Na^+. Conversely, the major astrocytic NKA (α2β2) is substantially saturated by intracellular Na^+ and ready to respond to $[K^+]_e$, for which it has low affinity. Moreover, α2β2 is sensitive to depolarization, whereas α3β1 is not (33, 42), and the astrocytic membrane potential is four times more sensitive to $[K^+]_e$ than that of neurons (43). The compounded result is that the astrocytic NKA is 18 times more sensitive to $[K^+]_e$ than the neuronal NKA (22). Synaptic activity causes astrocytic swelling (34), which is largely explained by the influx of Na^+ and bicarbonate via the electrogenic Na^+/HCO_3^- cotransporter 1 (NBCe1) and by metabolic stimulation (44, 45). Part of the Na^+ for the NKA may be provided by voltage-sensitive Na^+ channels, transient receptor potential (TRP) channels, and the Na^+/Ca^{2+} exchanger (46–48).

Another mechanism of K^+ clearance is spatial buffering, with the diffusion into astrocytes and other glial cells facilitated by constitutively open Kir4.1 potassium channels (49). Spatial buffering is considered relevant in the highly polarized retina (50) but no longer relevant in brain tissue. The main roles of Kir4.1 in astrocytes and oligodendrocytes are to set the membrane potential, to limit the amplitude of the $[K^+]_e$ rise under high frequency stimulation, and to mediate the delayed release of K^+, which is then captured by neurons to complete the K^+ cycle (31, 35, 48, 51–53). Worth noting is that a buffering role for Kir4.1 channels was sometimes deduced upon sensitivity to Ba^{2+}, but given the membrane potential sensitivity of α2β2 (**Figure 2*b***), the astrocytic effects of Ba^{2+} might also be explained by NKA modulation. The Na^+-K^+-$2Cl^-$ cotransporter, once deemed to be a significant K^+ clearance mechanism, plays a role in developing astrocytes, glioma

NBCe1: electrogenic Na^+/HCO_3^- cotransporter 1; abundant in astrocytes, it transduces $[K^+]_e$ into cytosolic pH

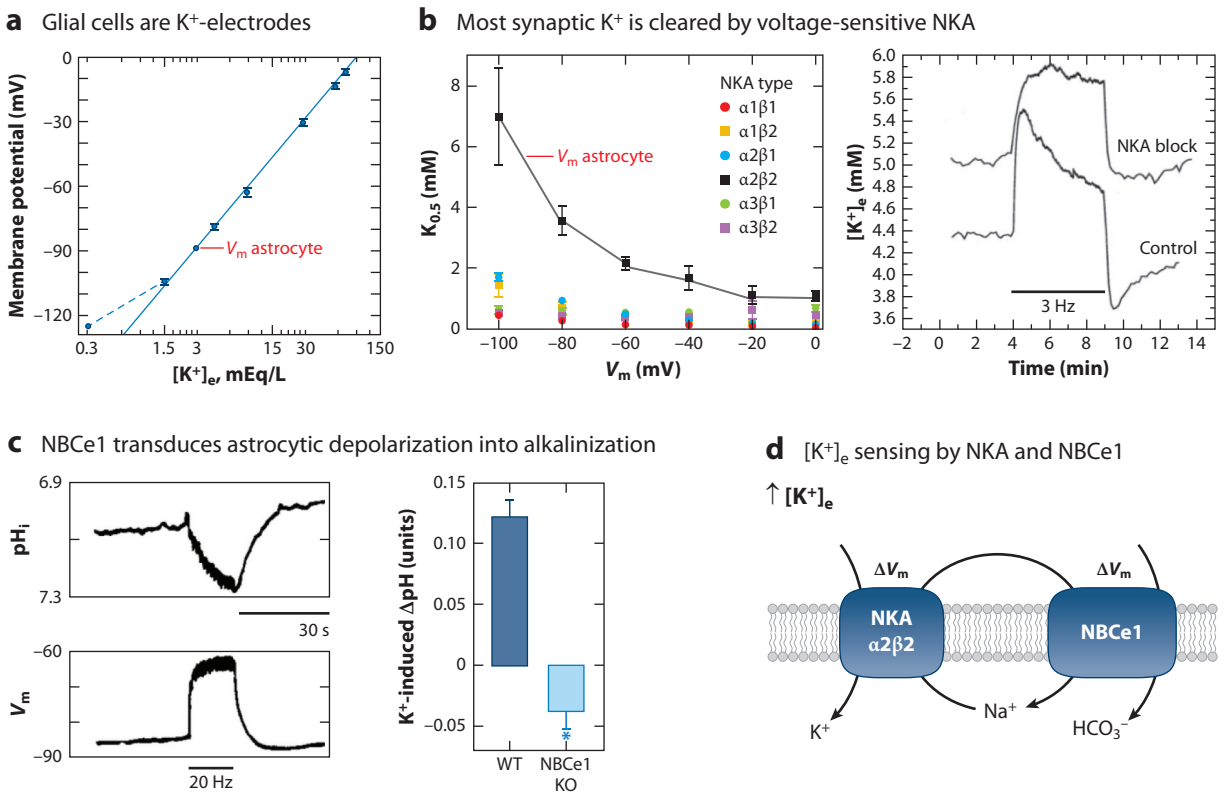

Figure 2

Extracellular K^+ ($[K^+]_e$) sensing by astrocytes. (*a*) Relation between $[K^+]_e$ and the glial membrane potential in the optic nerve of *Necturus*. The solid line has a slope of 59 mV according to the Nernst equation for a K^+-selective electrode. The typical resting membrane potential (V_m) of astrocytes is indicated. Panel adapted from Reference 39 (CC BY 4.0). (*b*, *left*) Voltage dependence of the K^+ half saturation constant ($K_{0.5}$) of rat Na^+/K^+ ATPase (NKA) isoform combinations expressed in *Xenopus laevis* oocytes, with α2β2 being the type found in mature astrocytes. The typical resting V_m of astrocytes is indicated. Panel adapted with permission from Reference 33; copyright 2014 Wiley. (*b*, *right*) Effect of neuronal stimulation (3 Hz) on hippocampal $[K^+]_e$, before (control) and during incubation with the NKA blocker dihydro-ouabain (5 μM). Panel adapted from Reference 31 (CC BY 4.0). (*c*, *left*) Effect of surface brain stimulation (20 Hz) on the V_m and intracellular pH (pH_i) of cortical astrocytes measured with microelectrodes. Panel adapted with permission from Reference 54; copyright 1989 Society for Neuroscience. (*c*, *right*) Effect of elevated $[K^+]_e$ (3 to 15 mM) on the pH of astrocytes cultured from control wild-type (WT) and Na^+/HCO_3^- cotransporter (NBCe1) knockout (KO) mice. Panel adapted from Reference 57. (*d*) Elevated $[K^+]_e$ is sensed by astrocytes, directly via the K^+-transport site at the NKA α2β2, and indirectly via the voltage sensitivity of both the NKA α2β2 and the NBCe1. Na^+ entering though the NBCe1 is recycled by the NKA.

cells, and optic nerve but not in adult gray matter (35, 48). The revised role of the astrocytic NKA, versus Kir4.1 channels, in the clearance of synaptic K^+ means that astrocytes take a much larger share of the brain's energy budget than anticipated (22).

The second astrocytic surface sensor with metabolic significance is the NBCe1. This protein, which is abundantly expressed in astrocytes and equivalent glial cells from nematodes to mammals, mediates the simultaneous translocation of one Na^+ and two HCO_3^-. In resting astrocytes, the NBCe1 is close to thermodynamic equilibrium and therefore catalytically silent. Upon depolarization by elevated $[K^+]_e$, the NBCe1 takes up Na^+ and HCO_3^-. Na^+ is recycled by the NKA, and the HCO_3^- causes intracellular alkalinization (54–57) (**Figure 2*c***). The NBCe1 works in parallel with the NKA α2β2 to transduce elevated $[K^+]_e$ into a metabolic response (**Figure 2*d***).

PRIMARY METABOLIC RECRUITMENT

Early Dismissal of $[K^+]_e$ as a Metabolic Signal

Whereas the importance of local K^+ in neurovascular coupling has been recognized (48, 58–60), acceptance of its metabolic role has lagged. Ever since Louis Sokoloff and colleagues introduced brain mapping with isotopic 2-deoxyglucose (61, 62), questions were asked about the mechanisms underlying activity-dependent metabolism and their relationship with information processing. A first clue was the observation that in vitro electrical stimulation of the axon-rich neurohypophysis led to deoxyglucose-6-phosphate accumulation, which was abolished by ouabain (63). Pushed to its limit by means of tissue section trajectography, the 2-deoxyglucose method showed similar rates of glucose consumption in neurons and astrocytes (64), a surprising result given the ostensibly larger energy demand of neurons. Neurons do not thrive in isolation, and astrocytes are easier to culture and may be passaged to obtain the large numbers required by isotopic measurements; hence, the metabolism of astrocytes is better known than that of neurons. Applied to astrocyte cultures, the 2-deoxyglucose method showed that glucose consumption is sensitive to NKA inhibition. Significantly, the astrocytic NKA was found to respond well to intracellular Na^+ but little, or not at all, to $[K^+]_e$, even at pathophysiological levels observed in seizures and spreading depression (65–68). At the same time, Pellerin & Magistretti (14) observed substantial stimulation of 2-deoxyglucose uptake in cultured astrocytes that was mediated by glutamate via the Na^+/glutamate cotransporter, intracellular Na^+ accumulation, and NKA activation. The glutamate experiment was soon reproduced by Sokoloff and colleagues, who concluded that "the stimulation (of glycolysis) is due not to increased $[K^+]_e$ but rather to another mechanism, such as the release of glutamate and/or possibly other neurotransmitters that promote Na^+ entry into the cells" (67, p. 4620). As elsewhere, the astrocytic NKA was assumed to be driven by intracellular Na^+, with K^+ being dismissed as a permissive cofactor; hence, its still popular short name is Na^+ pump, as opposed to K^+ pump.

Acute Modulation of Astrocytic Energy Metabolism by $[K^+]_e$

There is now evidence that the reported insensitivity of astrocytic metabolism to K^+ was an artifact. Astrocytes cultured in the absence of neurons, as required for the 2-deoxyglucose assay, fail to express $\alpha 2\beta 2$ (69, 70), which is the type of NKA that confers sensitivity to $[K^+]_e$ and to depolarization (33, 40–42). In addition, the trophic presence of neurons is required for the correct metabolic maturation of astrocytes (71, 72), and for practical reasons some studies used 5.4 mM as resting $[K^+]_e$ instead of the 2.5–3 mM prevalent in brain interstice. Thus, these resting astrocytes were already stimulated by K^+. Demonstration of the metabolic importance of $[K^+]_e$ had to wait for real-time assays capable of probing astrocytic transport and metabolism in the presence of neurons. Förster or fluorescence resonance energy transfer (FRET) microscopy used with a genetically encoded FRET sensor for glucose (73; see the sidebar titled Visualizing Metabolism)

VISUALIZING METABOLISM

Genetically encoded fluorescent sensors are giving fresh impetus to the study of metabolism and its regulation. These sensors are fusion proteins composed of one or two fluorescent proteins and a ligand-binding protein, typically a bacterial periplasmic protein or transcription factor. Binding of the ligand, e.g., glucose, induces a change in fluorescence that is detected by microscopy. Usually expressed by means of viral vectors, these minimally invasive tools can monitor metabolite levels within identified cells and subcellular organelles in real time, in vitro and in vivo. A comprehensive review of the more than 50 metabolite sensors that have been validated in mammalian cells, as well as their strengths and pitfalls, is available (148). Once the turf of biochemists, metabolism is becoming a subject of interest for cell physiologists.

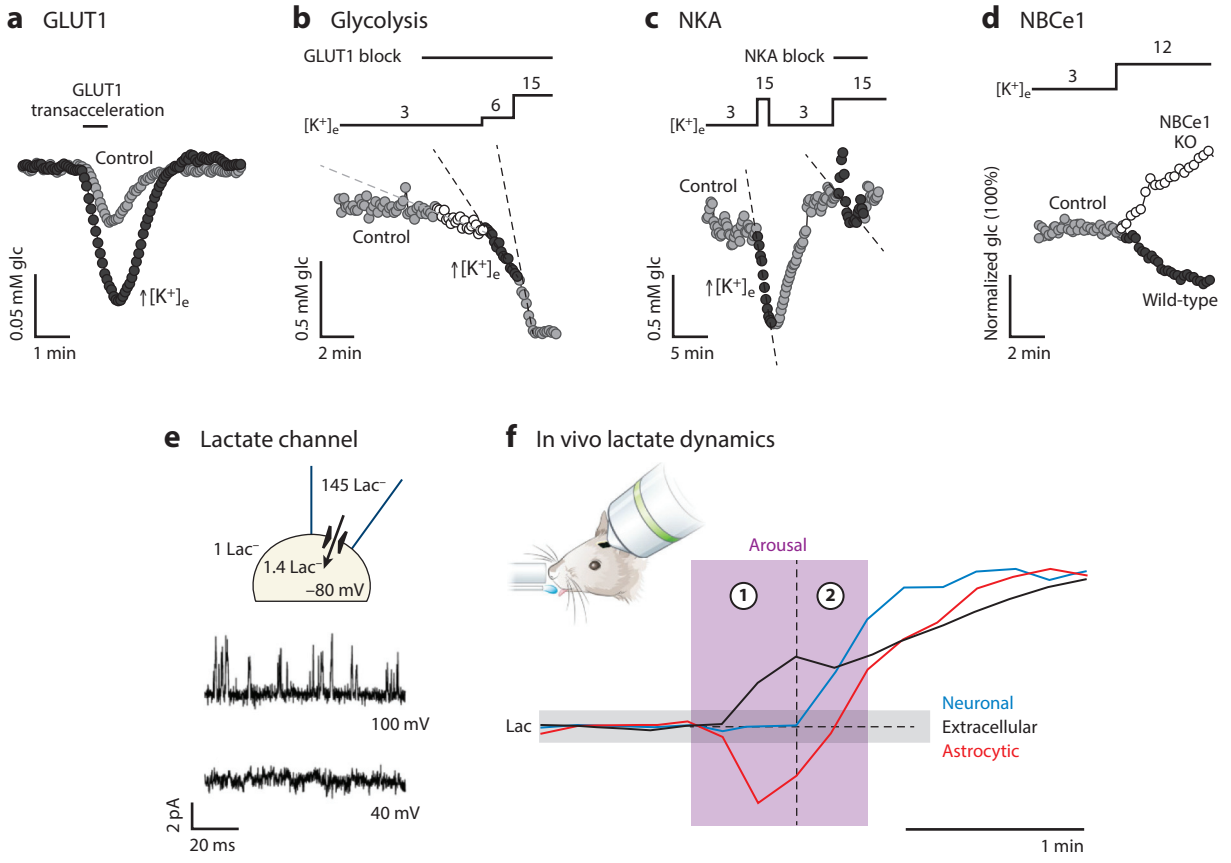

Figure 3

Metabolic effectors of elevated extracellular K^+ ($[K^+]_e$) in mouse astrocytes. (*a*) Glucose transporter isoform 1 (GLUT1) permeability, estimated as the rate of glucose transacceleration (accelerated exchange) induced with 3-*O*-methylglucose, was stimulated when $[K^+]_e$ was increased from 3 mM (*gray circles*) to 12 mM (*black circles*). Cytosolic glucose (glc) was measured with a genetically encoded Förster or fluorescence resonance energy transfer (FRET) sensor for glucose. Panel adapted from Reference 74. (*b*) The speed of glycolysis was measured in a cultured mouse astrocyte with the same sensor used in panel *a* as the rate of glc depletion induced by GLUT1 blockage with cytochalasin B (20 μM). Exposure to elevated $[K^+]_e$ (in mM) stimulated glucose consumption in a dose-dependent manner. Panel adapted from Reference 19. (*c*) The stimulation of glycolysis in a cultured mouse astrocyte caused rapid glucose depletion, which was curtailed in the presence of the Na^+/K^+ ATPase (NKA) blocker ouabain (1 mM). Panel adapted from Reference 19. (*d*) Glucose depletion induced by elevated $[K^+]_e$ in wild-type mice reverted to a glucose rise in Na^+/HCO_3^- cotransporter (NBCe1) knockout (KO) mice. Panel adapted from Reference 57. The rise is likely explained by unopposed GLUT1 stimulation (74). (*e*) Cell-attached patch-clamp recording of an astrocyte showing lactate (Lac) currents. Panel adapted from Reference 99. (*f*) Astrocytic, neuronal, and extracellular lactate were measured in the somatosensory cortex of an awake mouse using a genetically encoded FRET sensor for lactate and a microelectrode. Arousal induced by an isoflurane pulse (1.5%) led to astrocytic lactate depletion and extracellular lactate accumulation, which were followed by neuronal lactate accumulation. Panel adapted from Reference 83.

and in a minimally invasive protocol based on substrate transacceleration showed that elevated $[K^+]_e$ stimulated the astrocytic glucose transporter 1 (GLUT1) (74) (**Figure 3*a***). Whether or not astrocytes control the delivery of blood-borne glucose to neurons is not clear, as it is determined by how much of the capillary is covered by astrocytic endfeet (75, 76), a measurement that has been challenging (7, 77). Glycolysis can also be studied with a FRET glucose sensor. In this case, cells are first exposed to a GLUT1 blocker, leading to a steady decrease in cytosolic glucose as

hexokinase phosphorylates the hexose (78). Applying this transport-stop assay, researchers found that elevated $[K^+]_e$ stimulated the glycolytic rate of cultured astrocytes by more than 300% within seconds (19, 57, 79) (**Figure 3*b***). Confirmed in brain tissue slices (79–81) and associated with rapid lactate fluctuations in awake animals (82, 83), the astrocytic effect of K^+ is a strong candidate to explain the intriguing phenomenon of aerobic glycolysis (84, 85).

GLUT1: glucose transporter 1 is an isoform of the facilitative glucose transporter expressed in astrocytes, oligodendrocytes, and endothelial cells; neurons mainly express GLUT3

$[K^+]_e$ Is Transduced into a Metabolic Signal by the NKA and NBCe1

Consistent with NKA involvement, the stimulation of astrocytic glycolysis by K^+ is blocked by ouabain (19) (**Figure 3*c***). The mechanistic link between the pump and glycolytic machinery is not obvious. According to classic biochemistry, glycolysis is primarily regulated by adenine nucleotides, and ATP is indeed depleted in glutamate-treated astrocytes (80, 86, 87). However, in astrocytes exposed to elevated $[K^+]_e$, ATP levels actually rise (80, 88), which means that adenine nucleotides are not the signal between the astrocytic NKA and K^+-stimulated glycolysis. This nagging knowledge gap between the transduction of extracellular signals at the cell surface and the metabolic machinery is also present in neurons (1, 89). In addition to NKA $\alpha 2\beta 2$ engagement, the stimulation of astrocytic glycolysis by $[K^+]_e$ requires coactivation of the NBCe1, as demonstrated in culture and tissue slices by functional, pharmacological, and genetic means (57, 79) (**Figure 3*d***). The strong glycolytic response to cytosolic alkalinization by means other than K^+ (57), the exquisite in vitro pH sensitivity of phosphofructokinase (90), and the alkalinization of astrocytes in response to neural activity recorded in vivo (54, 91) suggest that pH may have an important role in the stimulation of glycolysis by elevated $[K^+]_e$. A recent in vivo study showed that subpopulations of cortical astrocytes may be defined based on whether they respond to physiological afferent stimulation with alkalinization or with acidification (92). $[K^+]_e$, acting via the NBCe1 and the HCO_3^--responsive soluble adenylyl cyclase, was proposed to mobilize glycogen (93), but the pharmacology that supports this possibility has been challenged (94). Glycogen mobilization by cAMP requires a coincidental Ca^{2+} rise (95, 96), which is not present in K^+-stimulated astrocytes (48), so the soluble adenylyl cyclase pathway may perhaps be more relevant in glutamate-stimulated astrocytes, which do mobilize Ca^{2+}. The metabolic role of the NBCe1 goes beyond K^+, as the rise in cytosolic NADH elicited by glutamate and ATP is also sensitive to functional and pharmacological inhibition of NBCe1 (81).

The Astrocytic Lactate Reservoir Is Mobilized by $[K^+]_e$

Astrocytes maintain higher steady-state lactate levels than neurons (97), a gradient also observed between glial cells and neurons in *Drosophila* (98). In cultured astrocytes, this lactate reservoir is acutely mobilized by elevated $[K^+]_e$, via a 37-pS, lactate-permeable anion channel that is gated by depolarization and extracellular lactate (99) (**Figure 3*e***). The lactate channel, which is yet to be identified at the molecular level, moves lactate 1,000 times faster than monocarboxylate transporter 1 (MCT1) and 4 (MCT4), the isoforms of the H^+-lactate symporter identified in astrocytes. Unlike MCTs, which are electroneutral, the lactate channel is capable of extruding lactate against a tenfold concentration gradient, using the membrane potential as a driving force. Expression of the channel may explain how mature astrocytes can export lactate efficiently despite the lack of detectable MCT4 messenger RNA (mRNA) expression (100) and the insensitivity of tissue lactate release to MCT blockers (101). A 1-mM rise in $[K^+]_e$ was sufficient to cause a lactate dip via the lactate-permeable channel (99), thereby releasing the tonic inhibition of glycolysis by the metabolite (102). Lactate may also be released by astrocytes via pannexin hemichannels in an activity-dependent fashion and in response to hypoxia (101). In awake mice under two-photon microscopy, the astrocytic lactate dip elicited by arousal was found to coincide with the

extracellular lactate surge that accompanies neural activity (82, 83, 103). These immediate responses were followed by sequential increases in astrocytic and neuronal lactate, respectively explained by glycolytic stimulation in astrocytes and lactate influx in neurons (**Figure 3*f***).

Crabtree effect: inhibition of mitochondrial respiration by glucose, which in astrocytes is triggered by high $[K^+]_e$

Mitochondrial Modulation by $[K^+]_e$

The most recently identified metabolic target of $[K^+]_e$ is the mitochondrion (80). Within seconds of exposure, the oxygen consumption of cultured astrocytes was reduced by 30% alongside a parallel reduction in mitochondrial pyruvate consumption. In hippocampal slices preincubated with tetrodotoxin to block the neuronal response, the inhibition of astrocytic respiration was evident as a rise in tissue oxygen level in response to elevated $[K^+]_e$. Consistently, experiments in vivo have shown that genetic ablation of astrocytic NBCe1 transformed the activity-dependent oxygen rise into an oxygen dip (104).

In longer observation periods in vivo, astrocytic mitochondrial metabolism was reported to increase (105). The acute reduction in mitochondrial oxygen consumption was found to be secondary to the NBCe1-dependent stimulation of glycolysis described above, possibly acting via a reduced cytosolic ADP/ATP ratio. This type of aerobic glycolysis may be understood as a regulated variant of the Crabtree effect (**Figure 4**), a phenomenon present in yeast and tumor cells in which mitochondria are suppressed by the glycolytic flux. This differs from the Warburg effect, where a primary change in mitochondria leads to augmented glycolysis (106).

Additional Primary Recruiters

Other intercellular signals capable of exerting acute metabolic effects on astrocytes are ammonium (NH_4^+) and nitric oxide. Neurons produce as much NH_4^+ as glutamate, a stoichiometry dictated

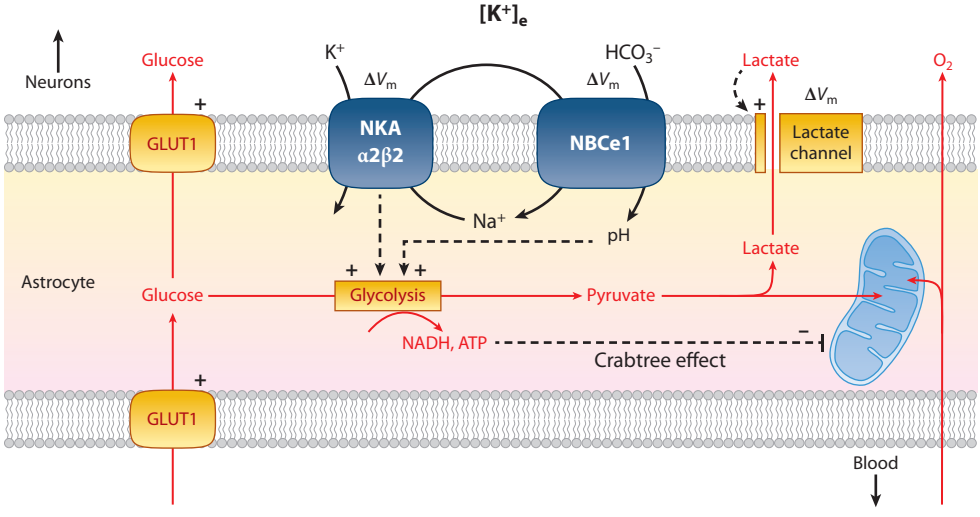

Figure 4

Modulation of astrocytic energy metabolism by extracellular K^+ ($[K^+]_e$). Glycolysis is stimulated by high $[K^+]_e$ via Na^+/K^+ ATPase (NKA) and Na^+/HCO_3^- contransporter 1 (NBCe1). Elevated $[K^+]_e$ also stimulates glucose transporter 1 (GLUT1) via an unknown mechanism, while triggering the opening of a lactate channel via depolarization and gating by extracellular lactate. The increased production of glycolytic ATP and NADH results in reduced oxygen consumption by mitochondria, a variant of the Crabtree effect. Overall, the metabolic effect of high $[K^+]_e$ on astrocytes is to increase the availability of lactate, glucose, and oxygen.

by the glutamate-glutamine cycle (107). It was once thought that the NH_4^+ resulting from the neuronal conversion of glutamine into glutamate might return to astrocytes in the form of amino acids, but that possibility has been challenged (108), whereas a substantial increase in neural tissue NH_4^+ is measured within seconds of stimulation (109–111). An important albeit neglected subject is the neuronal release of NH_4^+, via possible mechanisms such as its corelease with glutamate by synaptic vesicle fusion and its release via NH_4^+-permeable ion channels (112). NH_4^+ is similar in size and charge to K^+ and is a good substrate for the NKA, K^+ channels, and transporters (113, 114). The metabolic impact of NH_4^+ was recently studied with genetically encoded sensors in cultured cells and tissue slices. At physiological concentrations NH_4^+ was found to inhibit the uptake of pyruvate by astrocytic mitochondria, resulting in augmented lactate production, thus contributing to aerobic glycolysis (115). Nitric oxide is also capable of inhibiting astrocytic respiration (116), acutely and at physiological levels (117). Nitric oxide interferes directly with complex IV of the mitochondrial respiratory chain, resulting in augmented lactate production. Because the strongest source of nitric oxide in brain tissue is in the vascular endothelium, nitric oxide may contribute to refilling the astrocytic lactate reservoir while increasing the availability of oxygen for cells situated deeper in the parenchyma (117, 118). Future research will clarify how NH_4^+ and nitric oxide articulate with K^+ and glutamate, as well as with slow-acting factors like Wnt (119), brain-derived neurotrophic factor (120), and cannabinoids (121), to account for the complex metabolic changes required for sustained brain tissue performance and plasticity (82, 122–124).

In summary, the unique combination of strong NKA $\alpha 2\beta 2$ and NBCe1 expression in astrocytes makes glycolysis in these cells exquisitely sensitive to elevated $[K^+]_e$. In addition, elevated $[K^+]_e$ supports the glycolytic flux at both ends by delivering glucose via GLUT1 activation and by removing lactate via opening of the lactate channel. The result is accumulation of ATP and NADH, inhibition of mitochondrial respiration, and sparing of oxygen. This may be understood as a feed-forward regulatory mechanism whereby neurons use $[K^+]_e$ to recruit lactate, glucose, and oxygen when their energy demand is highest (**Figure 4**). The occurrence of aerobic glycolysis (84), i.e., glucose consumption in excess of oxygen consumption, may seem counterintuitive, as glycolysis is 15 times less efficient at producing ATP than oxidative phosphorylation. But the turnover time of oxygen is about 1 s, whereas that of glucose and lactate is measured in minutes (125). Aerobic glycolysis is not an efficient way to metabolize glucose but makes sense as a strategy to procure oxygen for active neurons. Consistent with this view, the local rise in tissue oxygen level that is observed during neural activity (126) reverted into an oxygen dip in NBCe1 knockout mice (104).

SECONDARY METABOLIC RECRUITMENT

Astrocytes located beyond the direct reach of high K^+ are also recruited. Neural activity decreases extracellular glucose (82, 127), creating a diffusional sink. If astrocytic glucose were also depleted, as suggested by results in culture and in tissue slices (19, 57, 79), additional glucose may be drawn in via gap junctions (128–130), a possibility awaiting the experimental demonstration of interastrocytic glucose gradients in vivo. Lactate may also be recruited. The astrocytic depletion of lactate near the active zone, which has been observed in culture, in slices and in awake animals, is predicted to create a sink. Lactate is negatively charged, and therefore its mobility toward the active zone should be further facilitated by the voltage gradient between resting astrocytes and depolarized astrocytes. The role of gap junctions in the delivery of lactate to support synaptic transmission and plasticity was found to be compromised by acute stress (131).

Lactate itself behaves as a secondary signal for metabolic recruitment. Lactate is released in a much wider region than K^+ and diffuses in the interstice for minutes instead of seconds (83, 132), so its distribution volume is much larger. When coincident with elevated $[K^+]_e$, lactate is actively

extruded from astrocytes (83, 99), which fosters their aerobic glycolysis by feedback derepression of glycolysis (102). In resting areas, i.e., beyond the reach of K^+, lactate reduces astrocytic and neuronal glucose consumption (1, 102), saving sugar for the active zone. Further sparing of fuel and oxygen may result from inhibition of neuronal activity through the G protein–coupled receptor HCAR1 (133–135). In contrast, the firing of active neurons is stimulated through positive modulation of the NMDA receptor by cytosolic NADH (136) and by spike facilitation mediated by the K_{ATP} channel (137). In addition, lactate was found to induce synapse-specific potentiation on cornu ammonis (CA3) pyramidal cells of the hippocampus through a cascade involving surface lactate receptors, G protein βγ subunits, inositol-1,4,5-trisphosphate 3-kinase, protein kinase C, and Ca^{2+}/calmodulin protein kinase II (CaMKII) (138).

A HIERARCHY OF METABOLIC COUPLING

Metabolic recruitment may be understood in the wider context of neurometabolic coupling (**Figure 5**). The lowest echelon is the intrinsic, cell-autonomous neuronal response, whereby

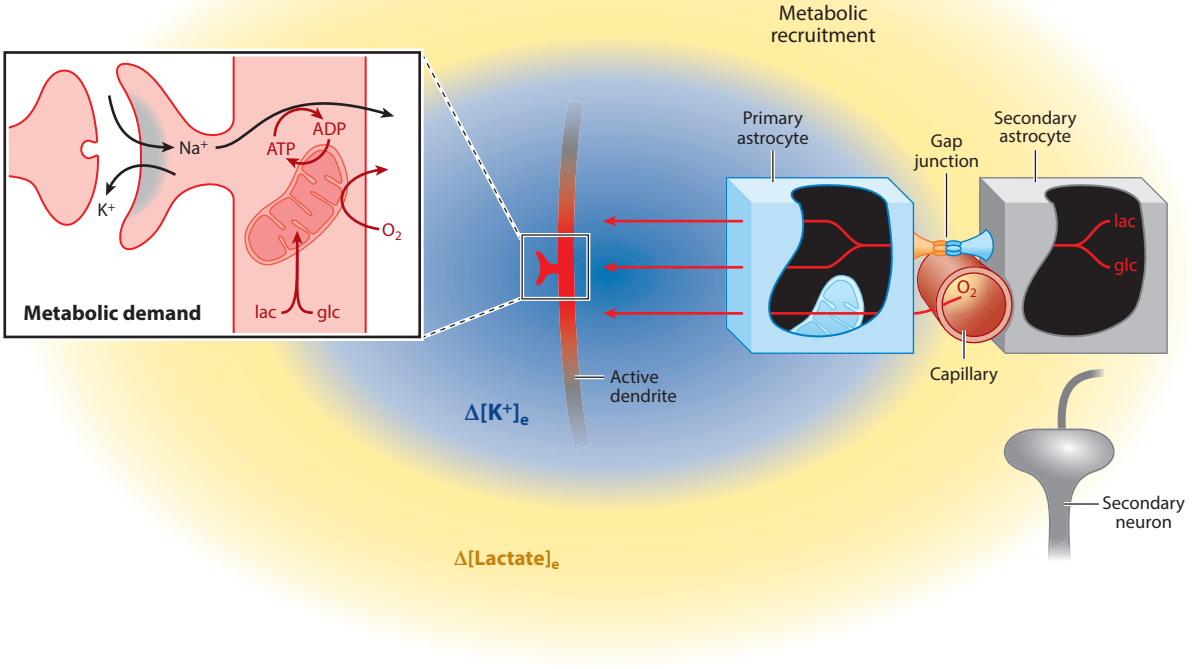

Figure 5

Primary and secondary metabolic recruitment. Excitatory postsynaptic potentials cause somatodendritic Na^+ accumulation and metabolic demand. Meanwhile, K^+ is released to the extracellular space. Elevated extracellular K^+ ($[K^+]_e$) modulates the metabolism of astrocytes, increasing the availability of lactate (lac), glucose (glc), and oxygen (primary recruitment). Lactate released by primary astrocytes inhibits the consumption of glucose by resting astrocytes and neurons and reduces the electrical activity of nonstimulated neurons (secondary recruitment). Reactive hyperemia further increases oxygen availability.

mitochondrial ATP production is quickly adjusted to the demand imposed by glutamate receptor ion channels via intracellular Na^+ and the NKA (1, 139) (see the inset in **Figure 5**). Superimposed to the neuronal response is metabolic recruitment. Here, postsynaptic neurons use K^+ acutely to harvest glucose, lactate, and oxygen from multiple astrocytes located beyond the active zone (primary recruitment). Depending on the neuronal compartment activated, K^+ is released via ionotropic receptors and/or K^+ channels. Distant resting astrocytes and neurons that lie beyond the reach of K^+ are recruited by lactate (secondary recruitment). The extended reach and short time course of metabolic recruitment are similar to those of the local vasodilation that underlies the blood-oxygen-level-dependent (BOLD) phenomenon and functional magnetic resonance imaging (126), in which $[K^+]_e$ is also a major player (48, 58–60). Minutes after these fast responses are over, glutamate transporter–mediated ANLS delivers lactate for long-lasting neuronal fueling and plasticity (14, 15, 19) (**Figure 5*b***). Similarly, the stimulation of the NMDA receptor of oligodendrocytes by glutamate caused GLUT1 translocation to the cell surface and augmented intracellular glucose with a half time of several minutes (140).

The energy consumption of the brain is remarkably flat, a difference of just 15% between deep sleep and wake. Nonetheless, individual neurons are known to increase their metabolic demand by several orders of magnitude. Macroscopic stability in the face of microscopic dynamism has been explained by several instances of averaging over space and time. One of them is lateral inhibition, where neurons actively inhibit neighboring neurons (141). A related concept is limited processing capacity (142), where the activation of a neuronal network is balanced by the inactivation of another. A near-infrared spectroscopy study in human subjects has provided a metabolic underpinning to this idea by showing that increased mitochondrial oxidative metabolism triggered by visual attention concurs with a reduction in mitochondrial metabolism associated with a parallel nonattended task (143). In view of the metabolic effects of K^+ and lactate, it seems reasonable to speculate that these signals may also be involved in setting the limits of brain tissue performance. Another strategy to cope with the large dynamic range of neurons is sparse coding, whereby information is encoded by only a few neurons at any given time (144, 145). And of course, there is neurovascular coupling, which recruits oxygen and fuel from the greater body reservoir (48, 58–60). Metabolic recruitment may be understood as a fundamental averaging strategy, working in parallel with lateral inhibition, competing network inactivation, sparse coding, and neurovascular coupling to sustain the ample dynamic range of individual neurons.

PERSPECTIVES

Following the mapping of the metabolic network in the heyday of classic biochemistry, radiolabeled metabolites helped to understand the gross compartmentation of metabolism and its idiosyncrasies in brain tissue (146, 147). The advent of genetically encoded fluorescent sensors and parallel progress in viral vector delivery and time-lapse microscopy have made it possible to monitor glucose, ATP, NADH, lactate, pyruvate, and other metabolites in identified cells and in real time (148). These tools have helped to unveil some of the rapid events described in this review, but we have not yet started to exploit their capabilities to investigate regional specializations (149), the behavior of subtypes of neurons and astrocytes (150), and the more subtle signaling events that evolve over prolonged periods of time (119–121). Even less is known about other types of glia and the many ways in which brain cells become dysfunctional (151, 152). Sensors for other metabolic pathways are being developed, and existing sensors are being improved, now built smaller for easier subcellular targeting and made of various colors for multiplexing (148). These technical developments herald an exciting era of metabolic physiology.

SUMMARY POINTS

1. Metabolic recruitment endows active neurons with the capability of harvesting fuel and oxygen from resting areas beyond the active zone.
2. The primary signal driving metabolic recruitment is elevated extracellular K^+ ($[K^+]_e$), which mirrors workload.
3. The energy metabolism of astrocytes is acutely modulated by $[K^+]_e$ via the Na^+/K^+ ATPase (NKA) and the Na^+/HCO_3^- cotransporter (NBCe1), proteins that are enriched in these cells.
4. Lactate released by astrocytes via ion channels serves as a secondary recruiter, impacting the function and metabolism of resting astrocytes and neurons.
5. Glutamate, ammonium (NH_4^+), and nitric oxide play supplementary roles over different spatiotemporal domains.
6. Metabolic recruitment works in parallel to other averaging strategies like lateral inhibition, competing network inactivation, sparse coding, and neurovascular coupling.

FUTURE ISSUES

1. What are the signaling pathways linking the NKA and NBCe1 to the metabolic machinery? This question reflects a more general knowledge gap about the control of metabolic pathways, including mitochondrial respiration.
2. What is the molecular identity of the astrocytic lactate channel? Are pannexin hemichannels active under physiological conditions?
3. NH_4^+ dynamics in brain tissue remain to be characterized; e.g., how and when do neurons release the NH_4^+ generated by the conversion of glutamine into glutamate?
4. In brain tissue, the capillary endothelium is a permeability barrier that controls the passage of glucose and lactate to the parenchyma. We know little about the regulation of brain endothelial glucose transporter 1 (GLUT1) and monocarboxylate transporters by neural activity.
5. Is there cellular and subcellular metabolic heterogeneity in neurons and glial cells?

DISCLOSURE STATEMENT

The authors are not aware of any affiliations, memberships, funding, or financial holdings that might be perceived as affecting the objectivity of this review.

ACKNOWLEDGMENTS

We thank Alejandro San Martín and Bruno Weber for inspiring conversations and Karen Everett for critically reading the manuscript. This work was partially funded by Fondecyt Grant 1200029 and ANID-BMBF Grant 180045 (to L.F.B.), Fondecyt Initiation Grant 11190678 (to I.R.), and an EMBO Long-Term Fellowship ALTF87-2018 (to I.F.-M.).

LITERATURE CITED

1. Baeza-Lehnert F, Saab AS, Gutierrez R, Larenas V, Diaz E, et al. 2019. Non-canonical control of neuronal energy status by the Na^+ pump. *Cell Metab*. 29:668–80
2. Heineman FW, Balaban RS. 1990. Phosphorus-31 nuclear magnetic resonance analysis of transient changes of canine myocardial metabolism in vivo. *J. Clin. Investig.* 85:843–52
3. Hochachka PW, McClelland GB. 1997. Cellular metabolic homeostasis during large-scale change in ATP turnover rates in muscles. *J. Exp. Biol.* 200:381–86
4. Steriade M, McCormick DA, Sejnowski TJ. 1993. Thalamocortical oscillations in the sleeping and aroused brain. *Science* 262:679–85
5. Attwell D, Laughlin SB. 2001. An energy budget for signaling in the grey matter of the brain. *J. Cereb. Blood Flow Metab.* 21:1133–45
6. Bushong EA, Martone ME, Jones YZ, Ellisman MH. 2002. Protoplasmic astrocytes in CA1 stratum radiatum occupy separate anatomical domains. *J. Neurosci.* 22:183–92
7. Mathiisen TM, Lehre KP, Danbolt NC, Ottersen OP. 2010. The perivascular astroglial sheath provides a complete covering of the brain microvessels: an electron microscopic 3D reconstruction. *Glia* 58:1094–103
8. Dringen R, Gebhardt R, Hamprecht B. 1993. Glycogen in astrocytes: possible function as lactate supply for neighboring cells. *Brain Res.* 623:208–14
9. Swanson RA. 1992. Physiologic coupling of glial glycogen metabolism to neuronal activity in brain. *Can. J. Physiol. Pharmacol.* 70(Suppl.):S138–44
10. Tsacopoulos M, Magistretti PJ. 1996. Metabolic coupling between glia and neurons. *J. Neurosci.* 16:877–85
11. Barros LF, Weber B. 2018. CrossTalk proposal: an important astrocyte-to-neuron lactate shuttle couples neuronal activity to glucose utilisation in the brain. *J. Physiol.* 596:347–50
12. Bonvento G, Bolanos JP. 2021. Astrocyte-neuron metabolic cooperation shapes brain activity. *Cell Metab.* 33:1546–64
13. Magistretti PJ, Allaman I. 2018. Lactate in the brain: from metabolic end-product to signalling molecule. *Nat. Rev. Neurosci.* 19:235–49
14. Pellerin L, Magistretti PJ. 1994. Glutamate uptake into astrocytes stimulates aerobic glycolysis: a mechanism coupling neuronal activity to glucose utilization. *PNAS* 91:10625–29
15. Loaiza A, Porras OH, Barros LF. 2003. Glutamate triggers rapid glucose transport stimulation in astrocytes as evidenced by real-time confocal microscopy. *J. Neurosci.* 23:7337–42
16. Erecinska M, Silver IA. 1994. Ions and energy in mammalian brain. *Prog. Neurobiol.* 43:37–71
17. Harris JJ, Jolivet R, Attwell D. 2012. Synaptic energy use and supply. *Neuron* 75:762–77
18. Rusakov DA, Kullmann DM. 1998. Extrasynaptic glutamate diffusion in the hippocampus: ultrastructural constraints, uptake, and receptor activation. *J. Neurosci.* 18:3158–70
19. Bittner CX, Valdebenito R, Ruminot I, Loaiza A, Larenas V, et al. 2011. Fast and reversible stimulation of astrocytic glycolysis by K^+ and a delayed and persistent effect of glutamate. *J. Neurosci.* 31:4709–13
20. Rangaraju V, Calloway N, Ryan TA. 2014. Activity-driven local ATP synthesis is required for synaptic function. *Cell* 156:825–35
21. Diaz-Garcia CM, Mongeon R, Lahmann C, Koveal D, Zucker H, Yellen G. 2017. Neuronal stimulation triggers neuronal glycolysis and not lactate uptake. *Cell Metab.* 26:361–74
22. Barros LF. 2022. How expensive is the astrocyte? *J. Cereb. Blood Flow Metab.* 42:738–45
23. Shih PY, Savtchenko LP, Kamasawa N, Dembitskaya Y, McHugh TJ, et al. 2013. Retrograde synaptic signaling mediated by K^+ efflux through postsynaptic NMDA receptors. *Cell Rep.* 5:941–51
24. Sykova E. 1983. Extracellular K^+ accumulation in the central nervous system. *Prog. Biophys. Mol. Biol.* 42:135–89
25. Frohlich F, Bazhenov M, Iragui-Madoz V, Sejnowski TJ. 2008. Potassium dynamics in the epileptic cortex: new insights on an old topic. *Neuroscientist* 14:422–33
26. Rasmussen R, Nicholas E, Petersen NC, Dietz AG, Xu Q, et al. 2019. Cortex-wide changes in extracellular potassium ions parallel brain state transitions in awake behaving mice. *Cell Rep.* 28:1182–94

27. Ding F, O'Donnell J, Xu Q, Kang N, Goldman N, Nedergaard M. 2016. Changes in the composition of brain interstitial ions control the sleep-wake cycle. *Science* 352:550–55
28. Armbruster M, Naskar S, Garcia JP, Sommer M, Kim E, et al. 2022. Neuronal activity drives pathway-specific depolarization of peripheral astrocyte processes. *Nat. Neurosci.* 25:607–16
29. Bergles DE, Jahr CE. 1997. Synaptic activation of glutamate transporters in hippocampal astrocytes. *Neuron* 19:1297–308
30. Lehre KP, Danbolt NC. 1998. The number of glutamate transporter subtype molecules at glutamatergic synapses: chemical and stereological quantification in young adult rat brain. *J. Neurosci.* 18:8751–57
31. D'Ambrosio R, Gordon DS, Winn HR. 2002. Differential role of KIR channel and Na^+/K^+-pump in the regulation of extracellular K^+ in rat hippocampus. *J. Neurophysiol.* 87:87–102
32. Larsen BR, Stoica A, MacAulay N. 2016. Managing brain extracellular K^+ during neuronal activity: the physiological role of the Na^+/K^+-ATPase subunit isoforms. *Front. Physiol.* 7:141
33. Larsen BR, Assentoft M, Cotrina ML, Hua SZ, Nedergaard M, et al. 2014. Contributions of the Na^+/K^+-ATPase, NKCC1, and Kir4.1 to hippocampal K^+ clearance and volume responses. *Glia* 62:608–22
34. Ransom BR, Yamate CL, Connors BW. 1985. Activity-dependent shrinkage of extracellular space in rat optic nerve: a developmental study. *J. Neurosci.* 5:532–35
35. MacAulay N. 2020. Molecular mechanisms of K^+ clearance and extracellular space shrinkage—glia cells as the stars. *Glia* 68:2192–211
36. Harik SI, Mitchell MJ, Kalaria RN. 1989. Ouabain binding in the human brain. Effects of Alzheimer's disease and aging. *Arch. Neurol.* 46:951–54
37. Bennay M, Langer J, Meier SD, Kafitz KW, Rose CR. 2008. Sodium signals in cerebellar Purkinje neurons and Bergmann glial cells evoked by glutamatergic synaptic transmission. *Glia* 56:1138–49
38. Langer J, Rose CR. 2009. Synaptically induced sodium signals in hippocampal astrocytes in situ. *J. Physiol.* 587:5859–77
39. Kuffler SW, Nicholls JG, Orkand RK. 1966. Physiological properties of glial cells in the central nervous system of amphibia. *J. Neurophysiol.* 29:768–87
40. Blanco G, Koster JC, Sanchez G, Mercer RW. 1995. Kinetic properties of the $\alpha2\beta1$ and $\alpha2\beta2$ isozymes of the Na, K-ATPase. *Biochemistry* 34:319–25
41. Crambert G, Hasler U, Beggah AT, Yu C, Modyanov NN, et al. 2000. Transport and pharmacological properties of nine different human Na, K-ATPase isozymes. *J. Biol. Chem.* 275:1976–86
42. Stanley CM, Gagnon DG, Bernal A, Meyer DJ, Rosenthal JJ, Artigas P. 2015. Importance of the voltage dependence of cardiac Na/K ATPase isozymes. *Biophys. J.* 109:1852–62
43. Hille B. 2001. *Ion Channels of Excitable Membranes*. Sunderland, MA: Sinauer Assoc.
44. Florence CM, Baillie LD, Mulligan SJ. 2012. Dynamic volume changes in astrocytes are an intrinsic phenomenon mediated by bicarbonate ion flux. *PLOS ONE* 7:e51124
45. Larsen BR, MacAulay N. 2017. Activity-dependent astrocyte swelling is mediated by pH-regulating mechanisms. *Glia* 65:1668–81
46. Black JA, Waxman SG. 2013. Noncanonical roles of voltage-gated sodium channels. *Neuron* 80:280–91
47. Sontheimer H, Fernandez-Marques E, Ullrich N, Pappas CA, Waxman SG. 1994. Astrocyte Na^+ channels are required for maintenance of Na^+/K^+-ATPase activity. *J. Neurosci.* 14:2464–75
48. Verkhratsky A, Nedergaard M. 2018. Physiology of astroglia. *Physiol. Rev.* 98:239–389
49. Orkand RK, Nicholls JG, Kuffler SW. 1966. Effect of nerve impulses on the membrane potential of glial cells in the central nervous system of amphibia. *J. Neurophysiol.* 29:788–806
50. Kofuji P, Newman EA. 2004. Potassium buffering in the central nervous system. *Neuroscience* 129:1045–56
51. Chever O, Djukic B, McCarthy KD, Amzica F. 2010. Implication of $K_{ir}4.1$ channel in excess potassium clearance: an *in vivo* study on anesthetized glial-conditional $K_{ir}4.1$ knock-out mice. *J. Neurosci.* 30:15769–77
52. Larson VA, Mironova Y, Vanderpool KG, Waisman A, Rash JE, et al. 2018. Oligodendrocytes control potassium accumulation in white matter and seizure susceptibility. *eLife* 7:e34829
53. Wallraff A, Kohling R, Heinemann U, Theis M, Willecke K, Steinhauser C. 2006. The impact of astrocytic gap junctional coupling on potassium buffering in the hippocampus. *J. Neurosci.* 26:5438–47

54. Chesler M, Kraig RP. 1987. Intracellular pH of astrocytes increases rapidly with cortical stimulation. *Am. J. Physiol.* 253:R666–70
55. Deitmer JW, Szatkowski M. 1990. Membrane potential dependence of intracellular pH regulation by identified glial cells in the leech central nervous system. *J. Physiol.* 421:617–31
56. Pappas CA, Ransom BR. 1994. Depolarization-induced alkalinization (DIA) in rat hippocampal astrocytes. *J. Neurophysiol.* 72:2816–26
57. Ruminot I, Gutierrez R, Peña-Munzenmeyer G, Añazco C, Sotelo-Hitschfeld T, et al. 2011. NBCe1 mediates the acute stimulation of astrocytic glycolysis by extracellular K^+. *J. Neurosci.* 31:14264–71
58. Filosa JA, Bonev AD, Straub SV, Meredith AL, Wilkerson MK, et al. 2006. Local potassium signaling couples neuronal activity to vasodilation in the brain. *Nat. Neurosci.* 9:1397–403
59. Attwell D, Buchan AM, Charpak S, Lauritzen M, MacVicar BA, Newman EA. 2010. Glial and neuronal control of brain blood flow. *Nature* 468:232–43
60. Hosford PS, Gourine AV. 2019. What is the key mediator of the neurovascular coupling response? *Neurosci. Biobehav. Rev.* 96:174–81
61. Sokoloff L, Reivich M, Kennedy C, Des Rosiers MH, Patlak CS, et al. 1977. The [^{14}C]deoxyglucose method for the measurement of local cerebral glucose utilization: theory, procedure, and normal values in the conscious and anesthetized albino rat. *J. Neurochem.* 28:897–916
62. Reivich M, Kuhl D, Wolf A, Greenberg J, Phelps M, et al. 1979. The [^{18}F] fluorodeoxyglucose method for the measurement of local cerebral glucose utilization in man. *Circ. Res.* 44:127–37
63. Mata M, Fink DJ, Gainer H, Smith CB, Davidsen L, et al. 1980. Activity-dependent energy metabolism in rat posterior pituitary primarily reflects sodium pump activity. *J. Neurochem.* 34:213–15
64. Nehlig A, Wittendorp-Rechenmann E, Lam CD. 2004. Selective uptake of [^{14}C]2-deoxyglucose by neurons and astrocytes: high-resolution microautoradiographic imaging by cellular ^{14}C-trajectography combined with immunohistochemistry. *J. Cereb. Blood Flow Metab.* 24:1004–14
65. Brookes N, Yarowsky PJ. 1985. Determinants of deoxyglucose uptake in cultured astrocytes: the role of the sodium pump. *J. Neurochem.* 44:473–79
66. Peng L, Zhang X, Hertz L. 1994. High extracellular potassium concentrations stimulate oxidative metabolism in a glutamatergic neuronal culture and glycolysis in cultured astrocytes but have no stimulatory effect in a GABAergic neuronal culture. *Brain Res.* 663:168–72
67. Takahashi S, Driscoll BF, Law MJ, Sokoloff L. 1995. Role of sodium and potassium ions in regulation of glucose metabolism in cultured astroglia. *PNAS* 92:4616–20
68. Yarowsky P, Boyne AF, Wierwille R, Brookes N. 1986. Effect of monensin on deoxyglucose uptake in cultured astrocytes: energy metabolism is coupled to sodium entry. *J. Neurosci.* 6:859–66
69. Brines ML, Robbins RJ. 1993. Cell-type specific expression of Na^+, K^+-ATPase catalytic subunits in cultured neurons and glia: evidence for polarized distribution in neurons. *Brain Res.* 631:1–11
70. Peng L, Arystarkhova E, Sweadner KJ. 1998. Plasticity of Na,K-ATPase isoform expression in cultures of flat astrocytes: species differences in gene expression. *Glia* 24:257–71
71. Hasel P, Dando O, Jiwaji Z, Baxter P, Todd AC, et al. 2017. Neurons and neuronal activity control gene expression in astrocytes to regulate their development and metabolism. *Nat. Commun.* 8:15132
72. Mamczur P, Borsuk B, Paszko J, Sas Z, Mozrzymas J, et al. 2015. Astrocyte-neuron crosstalk regulates the expression and subcellular localization of carbohydrate metabolism enzymes. *Glia* 63:328–40
73. Takanaga H, Chaudhuri B, Frommer WB. 2008. GLUT1 and GLUT9 as major contributors to glucose influx in HepG2 cells identified by a high sensitivity intramolecular FRET glucose sensor. *Biochim. Biophys. Acta* 1778:1091–99
74. Fernandez-Moncada I, Robles-Maldonado D, Castro P, Alegría K, Epp R, et al. 2020. Bidirectional astrocytic GLUT1 activation by elevated extracellular K^+. *Glia* 69:1012–21
75. Barros LF, Bittner CX, Loaiza A, Porras OH. 2007. A quantitative overview of glucose dynamics in the gliovascular unit. *Glia* 55:1222–37
76. Barros LF, San MA, Ruminot I, Sandoval PY, Fernandez-Moncada I, et al. 2017. Near-critical GLUT1 and neurodegeneration. *J. Neurosci. Res.* 95:2267–74
77. Korogod N, Petersen CC, Knott GW. 2015. Ultrastructural analysis of adult mouse neocortex comparing aldehyde perfusion with cryo fixation. *eLife* 4:e05793

78. Bittner CX, Loaiza A, Ruminot I, Larenas V, Sotelo-Hitschfeld T, et al. 2010. High resolution measurement of the glycolytic rate. *Front. Neuroenerget.* 2:26
79. Ruminot I, Schmalzle J, Leyton B, Barros LF, Deitmer JW. 2017. Tight coupling of astrocyte energy metabolism to synaptic activity revealed by genetically encoded FRET nanosensors in hippocampal tissue. *J. Cereb. Blood Flow Metab.* 39:513–23
80. Fernandez-Moncada I, Ruminot I, Robles-Maldonado D, Alegria K, Deitmer JW, Barros LF. 2018. Neuronal control of astrocytic respiration through a variant of the Crabtree effect. *PNAS* 115:1623–28
81. Kohler S, Winkler U, Sicker M, Hirrlinger J. 2018. NBCe1 mediates the regulation of the NADH/NAD^+ redox state in cortical astrocytes by neuronal signals. *Glia* 66:2233–45
82. Newman LA, Korol DL, Gold PE. 2011. Lactate produced by glycogenolysis in astrocytes regulates memory processing. *PLOS ONE* 6:e28427
83. Zuend M, Saab AS, Wyss MT, Ferrari KD, Hösli L, et al. 2020. Arousal-induced cortical activity triggers lactate release from astrocytes. *Nat. Metab.* 2:179–91
84. Fox PT, Raichle ME, Mintun MA, Dence C. 1988. Nonoxidative glucose consumption during focal physiologic neural activity. *Science* 241:462–64
85. Prichard J, Rothman D, Novotny E, Petroff O, Kuwabara T, et al. 1991. Lactate rise detected by ^1H NMR in human visual cortex during physiologic stimulation. *PNAS* 88:5829–31
86. Magistretti PJ, Chatton JY. 2005. Relationship between L-glutamate-regulated intracellular Na^+ dynamics and ATP hydrolysis in astrocytes. *J. Neural Transm.* 112:77–85
87. Lange SC, Winkler U, Andresen L, Byhro M, Waagepetersen HS, et al. 2015. Dynamic changes in cytosolic ATP levels in cultured glutamatergic neurons during NMDA-induced synaptic activity supported by glucose or lactate. *Neurochem. Res.* 40:2517–26
88. Lerchundi R, Kafitz KW, Winkler U, Farfers M, Hirrlinger J, Rose CR. 2019. FRET-based imaging of intracellular ATP in organotypic brain slices. *J. Neurosci. Res.* 97:933–45
89. Barros LF, San Martin A, Ruminot I, Sandoval PY, Baeza-Lehnert F, et al. 2020. Fluid brain glycolysis: limits, speed, location, moonlighting, and the fates of glycogen and lactate. *Neurochem. Res.* 45:1328–34
90. Trivedi B, Danforth WH. 1966. Effect of pH on the kinetics of frog muscle phosphofructokinase. *J. Biol. Chem.* 241:4110–12
91. Chesler M, Kraig RP. 1989. Intracellular pH transients of mammalian astrocytes. *J. Neurosci.* 9:2011–19
92. Theparambil SM, Hosford PS, Ruminot I, Kopach O, Reynolds JR, et al. 2020. Astrocytes regulate brain extracellular pH via a neuronal activity-dependent bicarbonate shuttle. *Nat. Commun.* 11:5073
93. Choi HB, Gordon GR, Zhou N, Tai C, Rungta RL, et al. 2012. Metabolic communication between astrocytes and neurons via bicarbonate-responsive soluble adenylyl cyclase. *Neuron* 75:1094–104
94. Jakobsen E, Andersen JV, Christensen SK, Siamka O, Larsen MR, et al. 2021. Pharmacological inhibition of mitochondrial soluble adenylyl cyclase in astrocytes causes activation of AMP-activated protein kinase and induces breakdown of glycogen. *Glia* 69:2828–44
95. Hertz L, Xu J, Song D, Du T, Li B, et al. 2015. Astrocytic glycogenolysis: mechanisms and functions. *Metab. Brain Dis.* 30:317–33
96. Hof PR, Pascale E, Magistretti PJ. 1988. K^+ at concentrations reached in the extracellular space during neuronal activity promotes a Ca^{2+}-dependent glycogen hydrolysis in mouse cerebral cortex. *J. Neurosci.* 8:1922–28
97. Machler P, Wyss MT, Elsayed M, Stobart J, Gutierrez R, et al. 2016. In vivo evidence for a lactate gradient from astrocytes to neurons. *Cell Metab.* 23:94–102
98. Gonzalez-Gutierrez A, Ibacache A, Esparza A, Barros LF, Sierralta J. 2019. Neuronal lactate levels depend on glia-derived lactate during high brain activity in *Drosophila*. *Glia* 68:1213–27
99. Sotelo-Hitschfeld T, Niemeyer MI, Machler P, Ruminot I, Lerchundi R, et al. 2015. Channel-mediated lactate release by K^+-stimulated astrocytes. *J. Neurosci.* 35:4168–78
100. Zhang Y, Chen K, Sloan SA, Bennett ML, Scholze AR, et al. 2014. An RNA-sequencing transcriptome and splicing database of glia, neurons, and vascular cells of the cerebral cortex. *J. Neurosci.* 34:11929–47

101. Karagiannis A, Sylantyev S, Hadjihambi A, Hosford PS, Kasparov S, Gourine AV. 2016. Hemichannel-mediated release of lactate. *J. Cereb. Blood Flow Metab.* 36:1202–11
102. Sotelo-Hitschfeld T, Fernandez-Moncada I, Barros LF. 2012. Acute feedback control of astrocytic glycolysis by lactate. *Glia* 60:674–80
103. Hu Y, Wilson GS. 1997. A temporary local energy pool coupled to neuronal activity: fluctuations of extracellular lactate levels in rat brain monitored with rapid-response enzyme-based sensor. *J. Neurochem.* 69:1484–90
104. Hosford PS, Wells JA, Ruminot I, Christie IN, Theparambil SM, et al. 2022. CO_2 signalling mediates neurovascular coupling in the cerebral cortex. *Nat. Comm.* 13:2125
105. Sonnay S, Poirot J, Just N, Clerc AC, Gruetter R, et al. 2018. Astrocytic and neuronal oxidative metabolism are coupled to the rate of glutamate-glutamine cycle in the tree shrew visual cortex. *Glia* 66:477–91
106. Barros LF, Ruminot I, San Martín A, Lerchundi R, Fernández-Moncada I, Baeza-Lehnert F. 2021. Aerobic glycolysis in the brain: Warburg and Crabtree contra Pasteur. *Neurochem. Res.* 46:15–22
107. Schousboe A, Scafidi S, Bak LK, Waagepetersen HS, McKenna MC. 2014. Glutamate metabolism in the brain focusing on astrocytes. *Adv. Neurobiol.* 11:13–30
108. Rothman DL, De Feyter HM, Maciejewski PK, Behar KL. 2012. Is there in vivo evidence for amino acid shuttles carrying ammonia from neurons to astrocytes? *Neurochem. Res.* 37:2597–612
109. Tashiro S. 1922. Studies on alkaligenesis in tissues. *Am. J. Physiol.* 60:519–43
110. Richter D, Dawson RM. 1948. The ammonia and glutamine content of the brain. *J. Biol. Chem.* 176:1199–210
111. Tsukada Y, Takagaki G, Sugimoto S, Hirano S. 1958. Changes in the ammonia and glutamine content of the rat brain induced by electric shock. *J. Neurochem.* 2:295–303
112. Marcaggi P. 2006. *An ammonium flux from neurons to glial cells*. Presented at the Physiological Society Main Meeting, London, UK
113. Kelly T, Rose CR. 2010. Ammonium influx pathways into astrocytes and neurones of hippocampal slices. *J. Neurochem.* 115:1123–36
114. Rangroo TV, Thrane AS, Wang F, Cotrina ML, Smith NA, et al. 2013. Ammonia triggers neuronal disinhibition and seizures by impairing astrocyte potassium buffering. *Nat. Med.* 19:1643–48
115. Lerchundi R, Fernandez-Moncada I, Contreras-Baeza Y, Sotelo-Hitschfeld T, Machler P, et al. 2015. NH_4^+ triggers the release of astrocytic lactate via mitochondrial pyruvate shunting. *PNAS* 112:11090–95
116. Almeida A, Moncada S, Bolanos JP. 2004. Nitric oxide switches on glycolysis through the AMP protein kinase and 6-phosphofructo-2-kinase pathway. *Nat. Cell Biol.* 6:45–51
117. San Martín A, Arce-Molina R, Galaz A, Perez-Guerra G, Barros LF. 2017. Nanomolar nitric oxide concentrations quickly and reversibly modulate astrocytic energy metabolism. *J. Biol. Chem.* 292:9432–38
118. Devor A, Sakadzic S, Saisan PA, Yaseen MA, Roussakis E, et al. 2011. "Overshoot" of O_2 is required to maintain baseline tissue oxygenation at locations distal to blood vessels. *J. Neurosci.* 31:13676–81
119. Cisternas P, Salazar P, Silva-Alvarez C, Barros LF, Inestrosa NC. 2016. Activation of Wnt signaling in cortical neurons enhances glucose utilization through glycolysis. *J. Biol. Chem.* 291:25950–64
120. Segarra-Mondejar M, Casellas-Diaz S, Ramiro-Pareta M, Muller-Sanchez C, Martorell-Riera A, et al. 2018. Synaptic activity-induced glycolysis facilitates membrane lipid provision and neurite outgrowth. *EMBO J.* 37:e97368
121. Jimenez-Blasco D, Busquets-Garcia A, Hebert-Chatelain E, Serrat R, Vicente-Gutierrez C, et al. 2020. Glucose metabolism links astroglial mitochondria to cannabinoid effects. *Nature* 583:603–8
122. Suzuki A, Stern SA, Bozdagi O, Huntley GW, Walker RH, et al. 2011. Astrocyte-neuron lactate transport is required for long-term memory formation. *Cell* 144:810–23
123. Goyal MS, Hawrylycz M, Miller JA, Snyder AZ, Raichle ME. 2014. Aerobic glycolysis in the human brain is associated with development and neotenous gene expression. *Cell Metab.* 19:49–57

124. Roumes H, Jolle C, Blanc J, Benkhaled I, Chatain CP, et al. 2021. Lactate transporters in the rat barrel cortex sustain whisker-dependent BOLD fMRI signal and behavioral performance. *PNAS* 118:e2112466118
125. Barros LF, San Martin A, Sotelo-Hitschfeld T, Lerchundi R, Fernandez-Moncada I, et al. 2013. Small is fast: astrocytic glucose and lactate metabolism at cellular resolution. *Front. Cell Neurosci.* 7:27
126. Ogawa S, Lee TM, Kay AR, Tank DW. 1990. Brain magnetic resonance imaging with contrast dependent on blood oxygenation. *PNAS* 87:9868–72
127. Hu Y, Wilson GS. 1997. Rapid changes in local extracellular rat brain glucose observed with an in vivo glucose sensor. *J. Neurochem.* 68:1745–52
128. Giaume C, Tabernero A, Medina JM. 1997. Metabolic trafficking through astrocytic gap junctions. *Glia* 21:114–23
129. Rouach N, Koulakoff A, Abudara V, Willecke K, Giaume C. 2008. Astroglial metabolic networks sustain hippocampal synaptic transmission. *Science* 322:1551–55
130. Clasadonte J, Scemes E, Wang Z, Boison D, Haydon PG. 2017. Connexin 43-mediated astroglial metabolic networks contribute to the regulation of the sleep-wake cycle. *Neuron* 95:1365–80
131. Murphy-Royal C, Johnston AD, Boyce AKJ, Diaz-Castro B, Institoris A, et al. 2020. Stress gates an astrocytic energy reservoir to impair synaptic plasticity. *Nat. Commun.* 11:2014
132. Heinemann U, Schaible HG, Schmidt RF. 1990. Changes in extracellular potassium concentration in cat spinal cord in response to innocuous and noxious stimulation of legs with healthy and inflamed knee joints. *Exp. Brain Res.* 79:283–92
133. Bozzo L, Puyal J, Chatton JY. 2013. Lactate modulates the activity of primary cortical neurons through a receptor-mediated pathway. *PLOS ONE* 8:e71721
134. de Castro AH, Briquet M, Schmuziger C, Restivo L, Puyal J, et al. 2019. The lactate receptor HCAR1 modulates neuronal network activity through the activation of Gα and Gβγ subunits. *J. Neurosci.* 39:4422–33
135. Herrera-Lopez G, Galvan EJ. 2018. Modulation of hippocampal excitability via the hydroxycarboxylic acid receptor 1. *Hippocampus* 28:557–67
136. Yang J, Ruchti E, Petit JM, Jourdain P, Grenningloh G, et al. 2014. Lactate promotes plasticity gene expression by potentiating NMDA signaling in neurons. *PNAS* 111:12228–33
137. Karagiannis A, Gallopin T, Lacroix A, Plaisier F, Piquet J, et al. 2021. Lactate is an energy substrate for rodent cortical neurons and enhances their firing activity. *eLife* 10:e71424
138. Herrera-Lopez G, Griego E, Galvan EJ. 2020. Lactate induces synapse-specific potentiation on CA3 pyramidal cells of rat hippocampus. *PLOS ONE* 15:e0242309
139. Barros LF, Baeza-Lehnert F. 2019. Perfect energy stability in neurons. *Aging* 11:6622–23
140. Saab AS, Tzvetavona ID, Trevisiol A, Baltan S, Dibaj P, et al. 2016. Oligodendroglial NMDA receptors regulate glucose import and axonal energy metabolism. *Neuron* 91:119–32
141. Hartline HK, Wagner HG, Ratliff F. 1956. Inhibition in the eye of Limulus. *J. Gen. Physiol.* 39:651–73
142. Navon D, Gopher D. 1979. On the economy of the human-processing system. *Psychol. Rev.* 86:214–55
143. Bruckmaier M, Tachtsidis I, Phan P, Lavie N. 2020. Attention and capacity limits in perception: a cellular metabolism account. *J. Neurosci.* 40:6801–11
144. Kording KP, Kayser C, Konig P. 2003. On the choice of a sparse prior. *Rev. Neurosci.* 14:53–62
145. Olshausen BA, Field DJ. 2004. Sparse coding of sensory inputs. *Curr. Opin. Neurobiol.* 14:481–87
146. Barros LF, Bolanos JP, Bonvento G, Bouzier-Sore AK, Brown A, et al. 2018. Current technical approaches to brain energy metabolism. *Glia* 66:1138–59
147. Barros LF, Brown A, Swanson RA. 2018. Glia in brain energy metabolism: a perspective. *Glia* 66:1134–37
148. San Martín A, Arce-Molina R, Aburto C, Baeza-Lehnert F, Barros LF, et al. 2022. Visualizing physiological parameters in cells and tissues using genetically encoded indicators for metabolites. *Free Radic. Biol. Med.* 182:34–58
149. Brancati GE, Rawas C, Ghestem A, Bernard C, Ivanov AI. 2021. Spatio-temporal heterogeneity in hippocampal metabolism in control and epilepsy conditions. *PNAS* 118:e2013972118

150. Zhang Y, Barres BA. 2010. Astrocyte heterogeneity: an underappreciated topic in neurobiology. *Curr. Opin. Neurobiol.* 20:588–94
151. Escartin C, Galea E, Lakatos A, O'Callaghan JP, Petzold GC, et al. 2021. Reactive astrocyte nomenclature, definitions, and future directions. *Nat. Neurosci.* 24:312–25
152. Le Douce J, Maugard M, Veran J, Matos M, Jego P, et al. 2020. Impairment of glycolysis-derived L-serine production in astrocytes contributes to cognitive deficits in Alzheimer's disease. *Cell Metab.* 31:503–17

RELATED RESOURCES

Brain RNA-Seq: **https://www.brainrnaseq.org/**. User friendly interphase to access cell type-specific transcriptomic data from human and mouse brain, provided by the Barres Lab. It also contains information about aging astrocytes, peritumor astrocytes, and microglia.